THE ASTROPHYSICAL JOURNAL, 258:53–58, 1982 July 1

CCD PHOTOMETRY OF MARKARIAN 421 AND 501

P. HICKSON,[1] G. G. FAHLMAN,[1] J. R. AUMAN, G. A. H. WALKER,[1] T. K. MENON,[1] AND Z. NINKOV
Department of Geophysics and Astronomy, University of British Columbia
Received 1981 September 14; accepted 1982 January 18

ABSTRACT

Observations of the BL Lacertae objects Markarian 501 and 421 have been made with a CCD detector at the prime focus of the 3.6 m Canada-France-Hawaii telescope. Each object was observed in two bands of FWHM $\approx$ 700 Å centered at 5000 Å and 6500 Å. Photometric profiles for both objects are presented and shown to be consistent with composite profiles from a point source and an elliptical galaxy which obeys the de Vaucouleurs surface brightness law. The derived photometric parameters of the underlying galaxies show them to be apparently normal elliptical galaxies.

Subject headings: BL Lacertae objects — galaxies: individual — galaxies: photometry

I. INTRODUCTION

The two galaxies, Markarian 421 and 501, discovered on the basis of their strong ultraviolet continuum (Markarian and Lipovotskii 1972) have been identified with the radio sources B2 1101+38 and B2 1652+39 (Colla *et al.* 1975) respectively. These galaxies exhibit the large optical polarization (Maza, Martin, and Angel 1978) and variability (Miller, McGimsey, and Williamon 1977) which is typical of BL Lacertae objects (Stein, O'Dell, and Strittmatter 1976). Both are X-ray sources (Rickets, Cooke, and Pounds 1976; Forman *et al.* 1978; Schwartz *et al.* 1978; Hearn, Marshall, and Jernigan 1979). Spectroscopic studies by Ulrich *et al.* (1975) show weak absorption lines which are characteristic of elliptical galaxies in an otherwise featureless spectrum. They derive redshifts of 0.0337 for Mrk 501 and 0.0308 for Mrk 421, although the latter is somewhat uncertain (Miller *et al.*). It is generally accepted that these are composite objects consisting of a compact, nonthermal variable source at the center of an elliptical galaxy. While this is a reasonable working hypothesis (see, e.g., Maza *et al.*), the structure of the underlying galaxies has heretofore only been studied with multi-aperture photometry (Kinman 1978; Mufson *et al.* 1980).

We have observed Mrk 421 and 501 with a CCD detector on the 3.6 m Canada-France-Hawaii telescope (CFHT) on Mauna Kea. Despite poor seeing, (1".7 FWHM) we are able to distinguish the galaxy from the central source. In this paper we present a brief discussion of the data reduction procedures used with our CCD and follow with an analysis of the surface brightness profiles of Mrk 421 and 501.

[1] Visiting Astronomer, Canada-France-Hawaii Telescope operated by the National Research Council of Canada, the Centre National de la Recherche Scientifique of France and the University of Hawaii.

II. OBSERVATIONS

Markarian 501 and 421 were observed on the nights of 1980 April 21 and 23, respectively, at the uncorrected prime focus of the CFHT. The detector used for these observations is a 100 × 100 element CCD manufactured in 1974 by the Bell Northern Research Corporation of Canada. It is a front-illuminated, surface-channel device with a broad spectral sensitivity peaking at about 6500 Å. The detector and its associated data acquisition system are described fully elsewhere (Hickson, Fahlman, and Walker 1981).

The standard passbands used in our system are defined by Corion broad-band interference filters. These have a roughly Gaussian transmission profile with a FWHM of 700 Å and center frequencies from 4000 Å to 10,000 Å at 500 Å intervals. We refer to these passbands with a two-digit subscript indicating the center frequency; e.g., λ_{50} is the passband centered at 5000 Å, F_{50} is the *mean* flux in this band (Jy), and I_{50} is the *mean* intensity in this band (Jy sr^{-1}).

Details of the observations are given in Table 1. In conjunction with each of these observations we obtained a star image to define the seeing profile and a sky exposure.

The reduction of the CCD photometry involves the following considerations:

1. *Flat fielding.*—Pixel response varies by about 5% across the array. To correct for this, our program images were divided by exposures of the dawn sky which we adopt as a flat field. Although the effective wavelengths of this calibration will differ somewhat from those of the observations, the flat field response of this CCD appears to vary little with color, judging from the λ_{50} and λ_{65} flat fields, which were quite repeatable and free from interference effects.

2. *Sky subtractions.*—Exposures on the sky were typically 5 minutes in length, and they were scaled to match the exposure times of the program images.

TABLE 1

OBSERVATIONAL LOG

Object	R. A. (1950)	Decl. (1950)	Filter	Exp. (s)	UT	Date
Mrk 501	$16^h52^m11^s.7$	+39°50′26″	λ_{50}	600	14.14	1980 Apr 21
			λ_{65}	600	14.30	1980 Apr 21
Mrk 421	11 01 40.6	+38 28 43	λ_{50}	300	06.50	1980 Apr 23
			λ_{65}	300	06.57	1980 Apr 23

3. *Cosmetic corrections.*—Incorrigible defects near the edges of the array limit its useful area to the central 92 × 66 pixels. Defects within this region are reasonably isolated and were corrected by interpolation. There is no evidence for cosmic-ray–induced noise events in any of our data. The pixels are not square, with dimensions of 28 μm × 32 μm (0″.43 × 0″.49 at the CFHT prime focus), and appropriate allowance for this was made in our reduction software.

4. *Charge transfer efficiency.*— At low light levels, the CCD suffers from charge transfer inefficiency. Light from the night sky generally provides enough bias charge to overcome this, but some charge transfer inefficiency was observed, particularly in the λ_{50} image of Mrk 421. The effect of this phenomenon is illustrated by the asymmetrical star images shown in the insets of Figures 1 and 2. We were able to compensate partially for this effect by running our observed images through a non-linear algorithm derived from the observed charge transfer efficiency versus charge curve for the CCD. If a site contains a charge Q and $f(Q)$ is transferred to the adjacent site by a single transfer, the transfer efficiency is $f(Q)/Q$. By considering the charge distribution arising from isolated point defects, we find $f(Q) \sim Q^{0.5}$ for our CCD. It is not difficult to show that in the absence of noise the image may be restored by simulating a second "readout" numerically using the inverse function $f^{-1}(Q)$ for each transfer. Unfortunately, the readout noise is amplified, which limits the usefulness of this kind of direct approach to reconstructing the image. We were unable to remove completely the charge transfer inefficiency from our data, but, as discussed in the next section, its effects on the results reported here are minor.

5. *Photometric calibration.*—The reduction to absolute flux was made by observing a number of equatorial photometric standards (Moffet and Barnes 1979; Landolt 1973) through our passbands and then applying the absolute calibrations of the V and R bands given by Johnson (1966). The conversion formula derived are:

$$V = -2.5 \log F_{50} + 8.95 + 0.83 \log (F_{50}/F_{65}), \quad (1)$$

and

$$R = -2.5 \log F_{65} + 8.70 + 0.83 \log (F_{50}/F_{65}). \quad (2)$$

The uncertainty is formally 0.02 mag but may actually be larger due to the limited number of standards with R-magnitudes. In addition, the effects discussed above limit the accuracy to about 0.1 mag at low light levels.

III. RESULTS

Contour maps of the λ_{65} images of Mrk 421 and 501 are shown in Figures 1 and 2 respectively. The images were smoothed prior to plotting by convolving them with a Gaussian filter with a half-width of $\sigma = 1.0$ pixel. Only the closed contours are plotted; the images do extend beyond the last contour shown. The stellar images shown on the same scale in the insets indicate the seeing profiles (and, as discussed previously, the asymmetry caused by charge transfer inefficiency). The outer contours of both objects have a modest ellipticity; $\epsilon = 0.3$ for Mrk 501 and $\epsilon = 0.2$ for Mrk 421. The low surface brightness companion of Mrk 421 has $\epsilon = 0.4$.

Surface brightness profiles for the objects were obtained as follows. The isophotal contours were used to define the effective radius, $r_* = (A/\pi)^{1/2}$, where A is the area enclosed by a given isophote (see Pritchet 1979 for a description of the algorithm used). The computation of r_* requires a complete isophotal contour, but, with the small field covered by our CCD, these are available only over a limited range of surface brightness. For an asymmetric galaxy the surface brightness profile defined by r_* is equivalent to that along cuts at the angles θ_* defined, relative to the major axis, by $\cos \theta_* = \pm(1 - e^2)^{1/2} e^{-1}$, where e is the eccentricity of the isophotes. With these cuts it is possible to extend the r_* profile beyond the limit of closed isophotal contours in a limited field. This simple prescription worked well in the case of Mrk 501 for which the surface brightness profile adopted is that defined by a cut through the nucleus at a position angle of 25° (measured CCW from north). In the case of Mrk 421, the image at low surface brightness is markedly asymmetric, an effect evidently due to the residual charge transfer inefficiency in our data. The adopted surface brightness profile is that along a cut taken at a position angle of 28° which we found to be the best match to the profile defined by the inner isophotes. The luminosity profiles in the specified directions were determined by a two-dimensional quadratic interpolation scheme applied to a smoothed image. The surface brightness profiles are shown in Figures 3 and 4 for Mrk 421 and 501 respectively.

We have modeled each object as an unresolved point source in a galaxy which has the luminosity profile of a de Vaucouleurs (1958) model, $\log (I/I_e) = -3.33 \times [(r_*/r_e)^{1/4} - 1]$, where I is the surface brightness, r_* is the effective radius, and I_e and r_e are constant parameters. The profile of the point source was

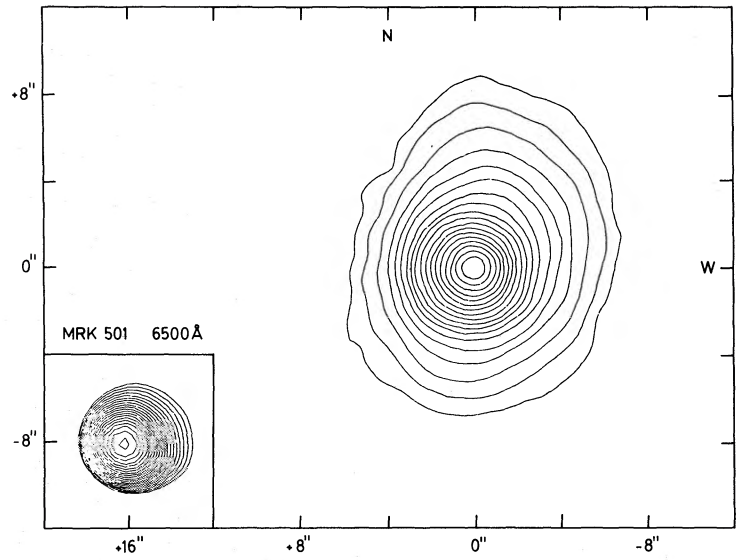

FIG. 1.—Contour map of Mrk 501. The contours are at intervals of 0.1 in log I_{65} with the outer contour at log $I_{65} = 6.03$ Jy sr^{-1}. The data have been smoothed with a Gaussian filter of width $\sigma = 1.0$ pixel. The inset shows a stellar profile at the same plate scale and contour spacing. North is at the top; east is to the left.

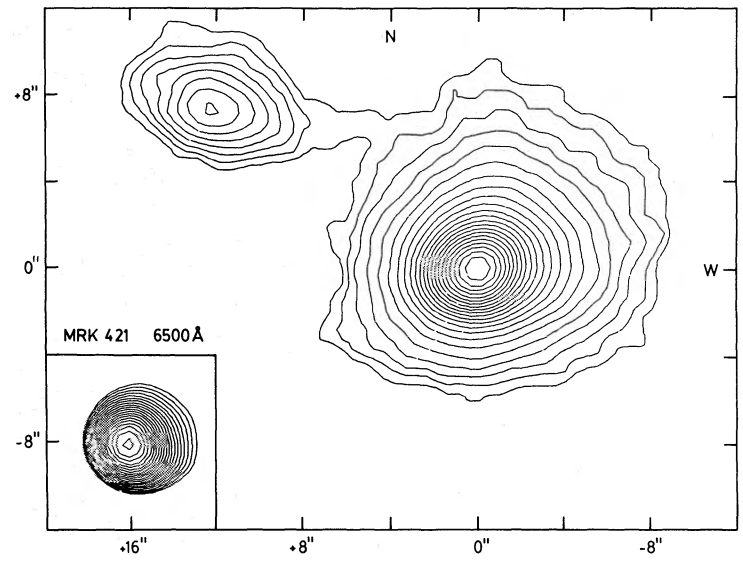

FIG. 2.—Contour map of Mrk 421 as in Fig. 1. The lowest contour is at log $I_{65} = 5.83$ Jy sr^{-1}.

determined from the star images acquired shortly after the galaxy observations. The adopted model components are shown in Figures 3 and 4 along with their sums. It is clear that they provide a good fit to the data.

We have also examined the fit of our surface brightness profiles to an exponential disk model for the underlying galaxy. In the case of Mrk 421, the fit of the exponential is quite inferior to that of the $r^{1/4}$ law, and there is little doubt that the underlying object is an elliptical galaxy. For Mrk 501, the exponential model fits about as well as the $r^{1/4}$ law in the region uncontaminated by the light from the nucleus. In considering this result we note that, because of the small field of our CCD, we are able to follow the surface brightness profile only over a distance roughly equal to the effective radius (r_e) of the de Vaucouleurs (1958) model. In other words, only one-half of the model galaxy luminosity is observed, and therefore one must regard the apparent good fit shown in Figure 4 with some caution. The exponential model, on the other hand, while having a smaller characteristic scale, is effectively defined over about 1 scale length as well because of the light contributions from the point source. Our image data do not permit an unambiguous choice to be made. However, we prefer to adopt the model of

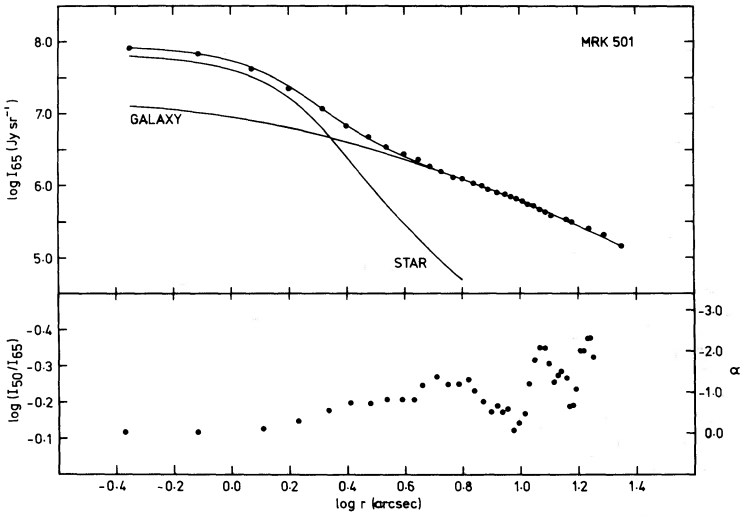

FIG. 3.—The surface brightness profile of Mrk 501 is shown in the upper panel and the color as a function of radius shown below. The curve labeled "Galaxy" is the adopted $r^{1/4}$ law corrected for seeing. The curve labeled "Star" is a stellar profile representing the light contribution from the unresolved nuclear source. The sum of these two components is the solid curve which runs through the indicated data points.

an elliptical galaxy because the photometric properties of the galaxy inferred from the model are quite consistent with other well-studied elliptical galaxies.

The parameters and integrated properties of the adopted model components are given in Table 2. The luminosity and magnitude values listed were obtained by integrating the models to an infinite radius. The spectral index listed for the stellar nucleus is based on the assumption that $F_\nu \sim \nu^{-\alpha}$, where the frequency baseline corresponds to our two bands at λ_{50} and λ_{65}.

Based on the fits of the observed surface brightness profiles to the model, we estimate that the measured values of r_e and $I_{e,65}$ are uncertain by about 2%. The corresponding error in the integrated luminosity is then about 6%. To these internal errors, must be added the uncertainty in the calibration, so that the integrated values quoted are uncertain by about 10%. The spectral index of the nonthermal component is very sensitive to even small errors in the log F_{50}/F_{65} ratio because of the small baseline.

IV. DISCUSSION

The composite nature of Mrk 421 and 501 has been recognized for some time. Previous efforts to study the characteristics of the host galaxy have all been based on aperture photometry. Kinman (1978) studied the surface brightness profiles derived from aperture photometry on both objects. Mufson *et al.* (1980) and Mufson (1982) used multi-aperture photometry to decompose Mrk 421 into a nonthermal point source and a host object which

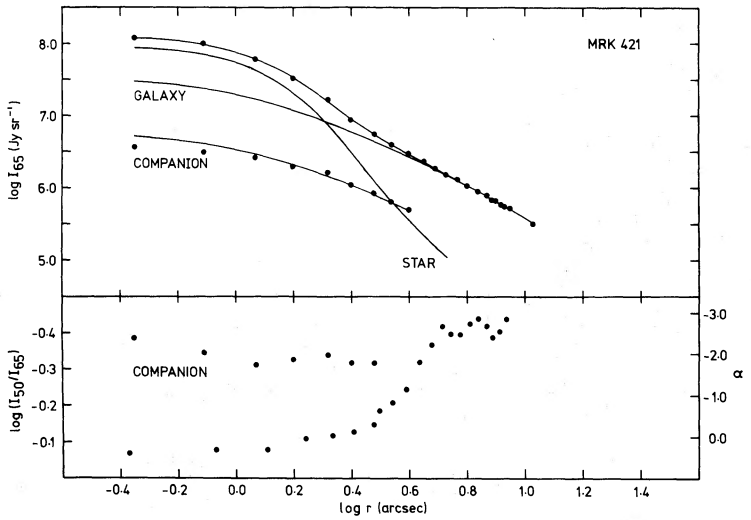

FIG. 4.—The surface brightness profile of Mrk 421 is shown as in Fig. 3

TABLE 2

STRUCTURAL AND PHOTOMETRIC PROPERTIES FROM MODEL FITS

PARAMETER	Mrk 501			Mrk 421			GALAXY
	Nucleus	Galaxy	Total	Nucleus	Galaxy	Total	
z	...	0.0337	...	...	0.0308	...	0.0316
r_e(arcsec)	...	16.68	...	...	8.03	...	3.98
log $I_{e,65}$ (Jy sr^{-1})	...	5.41	...	...	5.78	...	5.49
log F_{65} (Jy)	−2.34	−1.43	−1.38	−2.13	−1.69	−1.56	−2.58
log (F_{50}/F_{65})	−0.08	−0.25	−0.22	−0.02	−0.34	−0.23	−0.32
V	14.93	12.97	12.77	14.28	13.74	13.22	15.93
$V-R$	0.45	0.88	0.80	0.30	1.10	0.83	1.05
α	0.70	...	...	0.18	...	...	...

they assumed to be a giant elliptical. Maza, Martin, and Angel (1978, hereafter referred to as MMA) used the polarization of the nonthermal nuclear source and the assumption that the host galaxies have the colors expected for a normal giant elliptical to construct self-consistent composite models for both Mrk 421 and 501. A comparison of the results found by the above studies with our results is given in Table 3.

The agreement between our results and those of MMA is not too bad in view of the fact that MMA were forced to combine their polarization data through a 4″ aperture with published photometry taken through a 10″ aperture at different times to construct their models. For Mrk 501, our result agrees quite well with that of Kinman (1978), but the agreement is poor for Mrk 421. Kinman quotes a radius for the $V = 26.0$ isophote of 63″. The de Vaucouleurs law that fits our data (radius $\lesssim 10''$) gives a 42″ radius for this isophote. This size discrepancy might be due to contamination from the companion galaxy in the large apertures, although this would not account for the magnitude difference. This may indicate that the luminosity profile of Mrk 421 at large radii deviates from an extrapolation of the inner regions. Further observations should resolve this question. Our integrated V-magnitudes for both Mrk 421 and 501 agree well with those of Mufson (1982).

To assess the normalcy of the host galaxies we compare our results with the properties of the sample of elliptical galaxies studied thoroughly by Kormendy (1977). To effect the comparison, we must extrapolate our results to obtain B-magnitudes, and we also note that the K-correction is important at the redshifts of Mrk 421 and 501. We assume that the host galaxies have the normal $B-V$ colors of an elliptical galaxy given by Sandage (1973), and we also adopt the K-corrections listed by him. The resulting "zero redshift" magnitudes are given in Table 4.

For normal elliptical galaxies Kormendy (1977) showed that the surface brightness, $B_{0,e}$, at the effective radius r_e is correlated with r_e as follows:

$$B_{0,e} = 3.02 \log r_e + 19.74 , \quad (3)$$

with a standard deviation of 0.28. Substituting our values of r_e into this equation yields the predicted values shown in Table 4 which are to be compared with the values obtained by extrapolating our observed $I_{e,50}$. The agreement for both objects is excellent, which further supports the notion that the host galaxies are normal ellipticals.

An inspection of the results quoted in Table 2 shows that the most striking characteristic of Mrk 501 is its very large size—it has a value of r_e greater than any galaxy in the Kormendy (1977) sample. The size can perhaps be better appreciated if we note that the diameter at the 26.0 magnitude isophote is some 200 kpc (assuming $H = 50$ km s^{-1} kpc^{-1}). In view of the uncertainty

TABLE 3

COMPARISON OF UBC CCD IMAGE RESULTS WITH PREVIOUS MODELS

Observer	Parameter	Mrk 501	Mrk 421
MMA	$V(10'')$	14.35	14.38
UBC[a]	$V(10'')$	14.65	14.81
Mufson 1982	$V(12''.3)$	14.4	14.7
Mufson 1982	$V-R$	0.9	0.9
UBC	$V(12''.3)$	14.46	14.66
UBC	$V-R$	0.88	1.10
Kinman 1978	V_{26}	13.25	13.25
UBC	V_{26}	13.14	13.87

[a] UBC = University of British Columbia.

TABLE 4

PHOTOMETRIC PARAMETERS WITH K-CORRECTION

Parameter	Mrk 501	Mrk 421
V (observed)	12.97	13.74
$B-V$ (adopted)	1.09	1.08
B_e[a]	23.51	22.72
K_B (Sandage 1973)	0.16	0.15
$B_e - K_B$	23.35	22.57
B_e (eq. [3] of text)	23.41	22.33
M_B[b]	−22.51	−21.56

[a] This is the surface brightness (mag arcsec^{-2}) at the effective radius r_e and is extrapolated from the observed data with the adopted $B-V$ index.

[b] The absolute B-magnitude is based on the formula used by Kormendy 1977 as amended by Burstein 1979. It yields an absolute magnitude which is fainter than the integrated $r^{1/4}$ law by 0.11 mag.

inherent in extrapolating our fit to the de Vaucouleurs (1958) law, it would seem worthwhile to extend the surface brightness profile to larger distances to verify this result.

Markarian 421 appears to be anomalously red. Its $V-R$ index (including K-correction) is some 0.2 mag more positive than normal (Sandage 1973). It is interesting that the small companion to Mrk 421 has about the same $V-R$. The possible explanations include: (*a*) both galaxies are intrinsically red, (*b*) the distance to Mrk 421 is underestimated so that a larger K-correction is needed, and (*c*) there is a systematic error in our λ_{50} photometry, which effectively determines the V-magnitude, due to charge transfer inefficiency. The second explanation can be discounted because the redshift needed to make the $V-R$ color normal is so large ($z \approx 0.22$) that the object would be even more peculiar than it is already. The special circumstances implied by the first explanation are always difficult to discount, but it does seem implausible that both Mrk 421 and its companion would differ by $\sim 4\ \sigma$ from a normal $V-R$ color for elliptical galaxies. Thus, it would appear that the most reasonable explanation for the unusually red color we find for Mrk 421 is a small systematic error in our λ_{50} photometry due to charge transfer inefficiency. The λ_{50} image of Mrk 421 was the one most affected by charge transfer inefficiency, and the resulting photometry is thus somewhat uncertain. This suggests that the V-magnitude listed in Table 2 be decreased by ~ 0.2 mag. This change when carried over to the results in Table 3 actually improves the agreement with equation (3). Therefore, even if there is some suspicion that our V-magnitude (or more precisely, our λ_{50} photometry) for Mrk 421 is systematically too faint, our main conclusion, that the host is a normal elliptical, is unaffected.

In summary, the analysis of our CCD images of Mrk 421 and 501 confirms the common presumption that the host galaxies are apparently normal ellipticals. The interesting question, of course, is Why do these galaxies contain an abnormal nucleus? Evidently the pathology is not solely due to the internal structure of the galaxy. We note that both of these objects are very large, luminous, and undoubtedly massive galaxies which dynamically dominate their neighborhoods. Physical conditions in the local environment may be a crucial factor in the development of nuclear activity in such systems.

We are grateful to the CFHT staff for assistance at the telescope and to Ron Johnson for technical advice. This work was supported in part by the Natural Science and Engineering Research Council of Canada, and by a Canada Council Killam Scholarship and an NSERC University Research Fellowship to Paul Hickson.

REFERENCES

Burstein, D. 1979, *Ap. J.*, **234**, 435.
Colla, G., Fanti, C., Fanti, R., Giola, I., Lequeux, J., Lucas, R., and Ulrich, M.-H. 1975, *Astr. Ap. Suppl.*, **20**, 1.
de Vaucouleurs, G. 1958, in *Handbuch der Physik*, Vol. **53**, ed. S. Flügge (Berlin: Springer), p. 311.
Forman, W., Jones, C., Cominsky, L., Julien, P., Murray, S., Peters, G., Tananbaum, H., and Giacconi, R. 1978, *Ap. J. Suppl.*, **38**, 357.
Hearn, D. R., Marshall, F. J., and Jernigan, J. G. 1979, *Ap. J.* (*Letters*), **227**, L63.
Hickson, P., Fahlman, G. G., and Walker, G. A. H. 1981, *Proc. Soc. Photo-Opt. Instrum. Eng.*, **290**, 109.
Johnson, H. L. 1966, *Ann. Rev. Astr. Ap.*, **4**, 193.
Kinman, T. D. 1978, in *Pittsburgh Conference on BL Lac Objects*, ed. A. M. Wolfe (Pittsburgh: University of Pittsburgh), p. 82.
Kormendy, J. 1977, *Ap. J.*, **218**, 333.
Landolt, A. U. 1973, *A.J.*, **78**, 959.
Markarian, B. E., and Lipovetskii, V. A. 1972, *Astrofizika*, **8**, 155.
Maza, J., Martin, P. G., and Angel, J. R. P. 1978, *Ap. J.*, **224**, 368 (MMA).
Miller, H. R., McGimsey, B. W., and Williamon, R. M. 1977, *Ap. J.*, **217**, 382.
Moffet, T. J., and Barnes, T. G. 1979, *A.J.*, **84**, 627.
Mufson, S. L. 1982, private communication.
Mufson, S. L., *et al.* 1980, *Ap. J.*, **241**, 74.
Pritchet, C. 1979, *Ap. J.*, **231**, 354.
Ricketts, M. J., Cooke, B. A., and Pounds, K. A. 1976, *Nature*, **259**, 546.
Sandage, A. R. 1973, *Ap. J.*, **183**, 711.
Schwartz, D. A., Bradt, H. V., Doxsey, R. E., Griffiths, R. E., Gursky, H., Johnson, M. D., and Schwartz, J. 1978, *Ap. J.* (*Letters*), **224**, L103.
Stein, W. A., O'Dell, S. L., and Strittmatter, P. A. 1976, *Ann. Rev. Astr. Ap.*, **14**, 173.
Ulrich, M. H., Kinman, T. D., Lynds, C. R., Rieke, G. H., and Ekers, R. D. 1975, *Ap. J.*, **198**, 261.

J. R. AUMAN, G. G. FAHLMAN, P. HICKSON, T. K. MENON, Z. NINKOV, and G. A. H. WALKER: Department of Geophysics and Astronomy, University of British Columbia, Vancouver, B. C. V6T 1W5, Canada

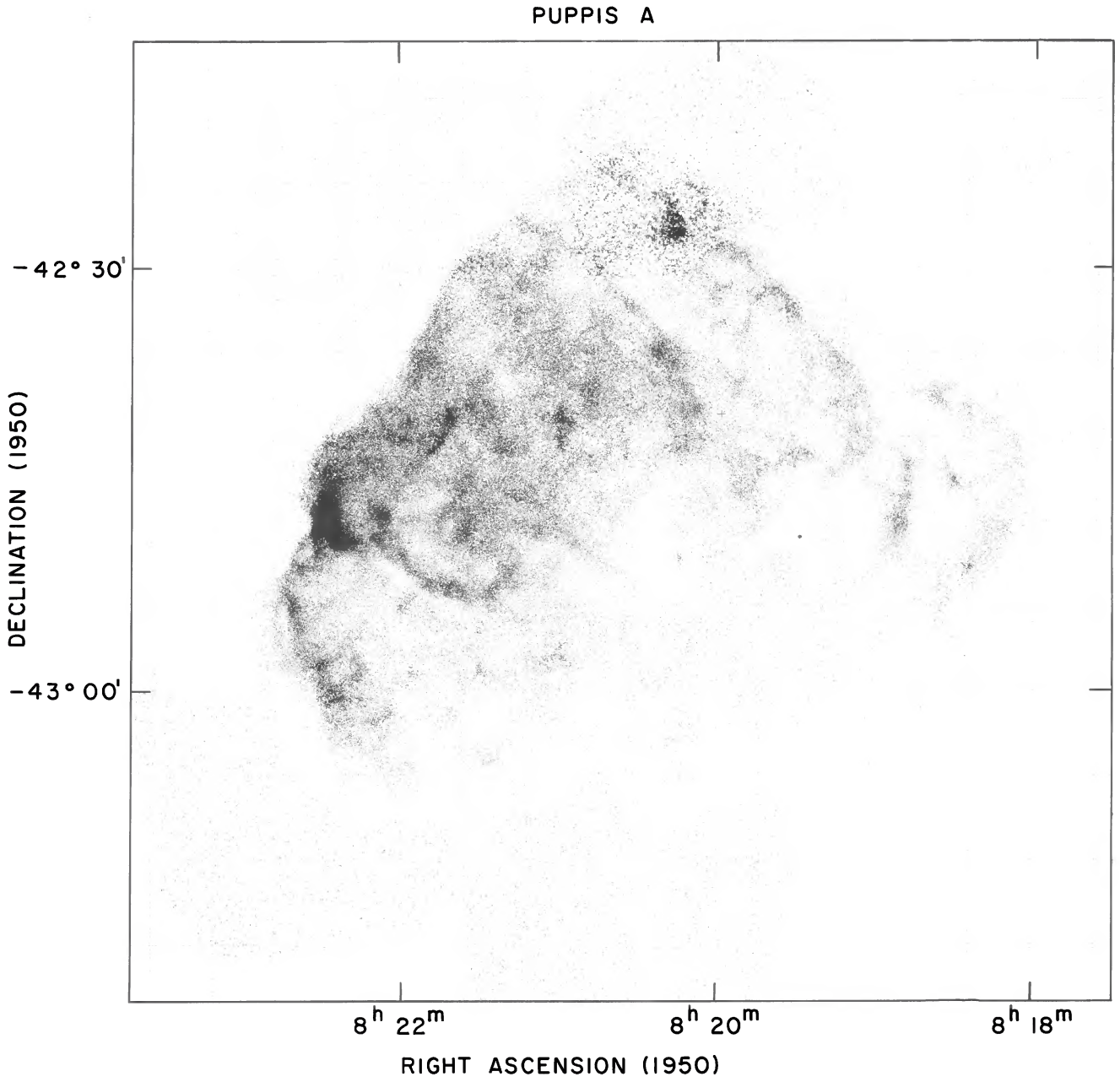

FIG. 2.—High resolution X-ray image of the Puppis A supernova remnant in energy range 0.1–4 keV. Map is an exposure-corrected photo-mosaic of 11 exposures taken by the *Einstein Observatory* HRI, binned in 8″ × 8″ pixels. The surface brightness scales linearly as the density of dots, with a threshold of 4×10^{-4} counts pixel^{-1} s^{-1} and a saturation level at 10^{-2} counts pixel^{-1} s^{-1}. The background rate is 10^{-4} counts pixel^{-1} s^{-1}.

PETRE *et al.* (*see* page 23)